

# A dynamical mean-field study of orbital-selective Mott phase enhanced by next-nearest neighbor hopping

Yuekun Niu<sup>1</sup>, Jian Sun<sup>1,2</sup>, Yu Ni<sup>1</sup>, Yun Song<sup>†1</sup>

<sup>1</sup>*Department of Physics, Beijing Normal University, Beijing 100875, China*

<sup>2</sup>*Beijing National Laboratory for Condensed Matter Physics, Institute of Physics, Chinese Academy of Sciences, Beijing 100190, China*

---

## Abstract

The dynamical mean-field theory is employed to study the orbital-selective Mott transition (OSMT) of the two-orbital Hubbard model with nearest neighbor hopping and next-nearest neighbor (NNN) hopping. The NNN hopping breaks the particle-hole symmetry at half filling and gives rise to an asymmetric density of states (DOS). Our calculations show that the broken symmetry of DOS benefits the OSMT, where the region of the orbital-selective Mott phase significantly extends with the increasing NNN hopping integral. We also find that Hund's rule coupling promotes OSMT by blocking the orbital fluctuations, but the influence of NNN hopping is more remarkable.

*Keywords:*

Dynamical mean-field theory, Two-orbital Hubbard model, Orbital-selective Mott transition, Next-nearest neighbor hopping

*PACS:* 71.27.+a, 71.30.+h, 72.80.Ga

---

## 1. Introduction

Mott metal-insulator transitions (MIT) in strongly correlated electron systems with orbital degrees of freedom has received much attention over the past decades [1, 2]. The orbital fluctuations tuned by the interactions may force the Mott MIT to happen successively in different orbitals, leading to the so-called orbital-selective Mott transition (OSMT) in the non-degenerated

---

*Email address:* yunsong@bnu.edu.cn (Yun Song<sup>†1</sup>)

multiorbital systems [2, 3]. In an orbital-selective Mott phase (OSMP), the carriers on a subset of orbitals get localized but others remain itinerant. This phenomenon has been observed experimentally in some transition-metal compounds, including the iron-based superconductors [4, 5].

Many theoretical methods have been employed to study the OSMT in multiorbital systems, including the quantum Monte Carlo technique [6], dynamical cluster approximation [7], slave-boson method [8], and dynamical mean-field theory (DMFT)[1, 9]. It is well known that the DMFT approach, which handles band-like and atomic-like aspects on equal footing, is an appropriate theoretical framework for the study of Mott MIT [10]. Combined with various impurity solvers, the DMFT approach has been used to study the OSMT in multiorbital systems with different energy scales. So far, three kinds of factors have been confirmed for the appearance of OSMT, including the Hund's rule coupling, crystal field splitting, and bandwidth differences among orbitals.

It has been proposed that Hund's rule coupling ( $J$ ) is indeed responsible for the correlation effects by strongly suppressing the coherence scale for the formation of a Fermi liquid [2]. The Hund's coupling promotes the OSMT at half filling [11, 12, 13], which can be understood by recognizing that  $J$  blocks orbital fluctuations [2]. Besides, the other two factors influence the OSMT by introducing the nondegeneration among the orbitals of multiorbitals system. The important role of the bandwidth difference in finding OSMT has been verified by the earlier DMFT investigations of the two-orbital Hubbard model with unequal bandwidths [14, 15, 16]. On the other hand, the orbital degeneracy can also be broken by the crystal field splitting, leading to OSMT in multiorbital systems [17, 18, 19, 20].

Apart from the three factors mentioned above, is there any other model parameter which also plays an essential role in the OSMT? In this study we concentrate on the influence of the next-nearest neighbor (NNN) hopping integrals. In some previous DMFT calculations [10], the randomness of the NNN hopping has been introduced to suppress antiferromagnetism in the half-filled Hubbard model at weak coupling. Under this condition, the density of states (DOS) remains semielliptic, and the Bethe lattice holds the particle-hole symmetry [21, 22]. However, it has been found that the DOS is no longer semielliptic in the tight-binding model with standard NNN hopping [23, 24]. Therefore, it is important to make it clear how the OSMT is influenced by the broken symmetry of DOS for multiorbital systems at half-filling.

In this paper we study the effect of NNN hopping on the OSMT in two-

orbital Hubbard model by using the DMFT approach with the Lanczos diagonalization method [25] as its impurity solver. The Lanczos solver is very powerful in finding the critical point of the Mott MIT, which has been proved to be far superior than some other impurity solvers [26, 27]. Because of the asymmetric DOS introduced by the NNN hopping, the calculations become more complicated. We have to adjust the value of chemical potential to construct the whole phase diagram of the two-orbital Hubbard model at half filling. By performing a large amount of numerical calculations, we investigate the evolution of phase diagram with the increasing of the NNN hopping integrals in the conditions with different Hund's rule coupling and also different nearest neighbor hopping ratio. We find that the region of OSMP significantly increases with the increasing NNN hopping amplitudes, indicating that the asymmetric DOS introduced by the NNN hopping plays a key role in the promotion of OSMT, in spite of the change of the bandwidth ratio. On the other hand, we also find that the orbital fluctuations are blocked with the increasing of Hund's rule coupling, leading the critical values of both narrow and wide band decrease manifestly. However, the enhancement of Hund's coupling on the OSMT is weaker than the effect of the NNN hopping.

## 2. Model and methodology

We study the extended two-orbital Hubbard model, where the hopping has both NN and NNN contributions. The Hamiltonian is expressed as

$$\begin{aligned}
H = & - \sum_l t_l \sum_{\langle ij \rangle \sigma} d_{il\sigma}^\dagger d_{jl\sigma} - \sum_l t'_l \sum_{\langle\langle ii' \rangle\rangle \sigma} d_{il\sigma}^\dagger d_{i'l\sigma} - \mu \sum_{il\sigma} d_{il\sigma}^\dagger d_{il\sigma} \\
& + \frac{U}{2} \sum_{il\sigma} n_{il\sigma} n_{il\bar{\sigma}} + \sum_{i\sigma\sigma'} (U' - \delta_{\sigma\sigma'} J) n_{i1\sigma} n_{i2\sigma'} \\
& + \frac{J}{2} \sum_{i,l \neq l',\sigma} (d_{il\sigma}^\dagger d_{il\bar{\sigma}}^\dagger d_{i'l'\bar{\sigma}} d_{i'l'\sigma} + d_{il\sigma}^\dagger d_{i'l'\sigma'}^\dagger d_{i'l\sigma'} d_{i'l'\sigma}), \tag{1}
\end{aligned}$$

where operator  $d_{il\sigma}^\dagger$  creates an electron with spin  $\sigma$  in orbital  $l$  of site  $i$ .  $\langle ij \rangle$  and  $\langle\langle ii' \rangle\rangle$  represent the summations over NN and NNN sites, and  $t_l$  and  $t'_l$  denote the NN and NNN hopping amplitudes for orbital  $l$ .  $U$  and  $U'$  are the intra-orbital and interorbital Coulomb interactions, and  $J$  is the Hund's rule coupling. The onsite component of Green's function for different

orbital  $l$  can be obtained by [10],

$$G_{ii}^{(l)}(\omega) = \sum_{\vec{k}} G_l(\vec{k}, \omega) = \int_{-\infty}^{+\infty} d\epsilon \frac{D_l^{t,t'}(\epsilon)}{\omega + \mu - \epsilon_l(\vec{k}) - \Sigma_l(\omega)}. \quad (2)$$

In the infinite limit  $Z \rightarrow \infty$ , the DOS of the Bethe lattice with both NN and NNN hopping can be expressed as [23]

$$D_l^{t,t'}(\epsilon) = \frac{\Theta[1 + 4K_l(K_l + \epsilon/t_l)]}{\sqrt{1 + 4K_l(K_l + \epsilon/t_l)}} \sum_{n=1}^2 \frac{\sqrt{4 - [\lambda_l^{(n)}]^2(\epsilon)}}{2\pi t_l}, \quad (3)$$

with

$$\begin{aligned} \lambda_l^{(1)}(\epsilon) &= \frac{-1 + \sqrt{1 + 4K_l(K_l + \epsilon/t_l)}}{2K_l}, \\ \lambda_l^{(2)}(\epsilon) &= \frac{-1 - \sqrt{1 + 4K_l(K_l + \epsilon/t_l)}}{2K_l}, \end{aligned} \quad (4)$$

where  $K_l = t'_l/t_l$  represents the ratio between NNN hopping  $t'_l$  and NN hopping  $t_l$  of orbital  $l$ . As the NNN hopping integrals increase,  $D_l^{t,t'}(\epsilon)$  becomes asymmetric and develops a square-root singularity at a band edge [23].

In the framework of DMFT, the Hubbard model is mapped into an Anderson impurity model (AIM),

$$\begin{aligned} H_{imp} &= \sum_{ml\sigma} \epsilon_{ml} c_{ml\sigma}^\dagger c_{ml\sigma} + \sum_{ml\sigma} V_{ml} (c_{ml\sigma}^\dagger d_{l\sigma} + d_{l\sigma}^\dagger c_{ml\sigma}) + \sum_{l\sigma} (\epsilon_l - \mu) d_{l\sigma}^\dagger d_{l\sigma} \\ &+ \frac{U}{2} \sum_{l\sigma} n_{l\sigma} n_{l\bar{\sigma}} + \sum_{\sigma\sigma'} (U' - \delta_{\sigma\sigma'} J) n_{1\sigma} n_{2\sigma'} + \frac{J}{2} \sum_{l \neq l', \sigma} d_{l\sigma}^\dagger d_{l'\bar{\sigma}}^\dagger d_{l'\sigma} d_{l\sigma} \\ &+ \frac{J}{2} \sum_{l \neq l', \sigma} d_{l\sigma}^\dagger d_{l'\sigma}^\dagger d_{l\sigma'} d_{l'\sigma}, \end{aligned} \quad (5)$$

where the parameter  $\epsilon_{ml}$  represents the energy of the  $m$ th environmental bath for the orbital  $l$ , and  $V_{ml}$  describes the couplings between the bathes and the impurity site.

We employ Lanczos exact diagonalization approach [25] as an impurity solver to calculate the Green's function ( $G_{AIM}^{(l)}$ ) and the self energy ( $\Sigma_{AIM}^{(l)}$ ) of AIM. The parameters  $\epsilon_{ml}$  and  $V_{ml}$  in AIM can be obtained self-consistently

by introducing  $G_{ii}^{(l)}(\omega) = G_{AIM}^{(l)}(\omega)$  and  $\Sigma_l(\omega) = \Sigma_{AIM}^{(l)}(\omega)$  [10]. In our DMFT calculations, the bath size is chosen as  $n_b = 3$ . In Table 1, we show the self-consistent values of the parameters of AIM for the metallic phase, OSMP and insulating phase, respectively.

Table 1: The values of the AIM parameters in the DMFT self-consistent calculations for different interactions  $U$  when  $t_2/t_1 = 0.5$ ,  $K = 0.5$ , and  $J/U = 0.5$ , corresponding to the metallic phase, orbital-selective Mott phase and insulating phase, respectively.

Metal ( $U = 0.01$ )	bath-1	bath-2	bath-3
$\epsilon_1$	1.498717	0.334170	-0.072524
$V_1$	0.862313	0.411842	0.423400
$\epsilon_2$	0.376248	-0.108999	0.005459
$V_2$	0.425066	0.171245	-0.109655
OSMP ( $U = 2.40$ )	bath-1	bath-2	bath-3
$\epsilon_1$	0.780082	0.100286	-0.015272
$V_1$	0.486443	0.195582	0.178468
$\epsilon_2$	1.435533	-0.875888	-0.280482
$V_2$	0.338925	0.269218	0.000639
Insulator ( $U = 4.40$ )	bath-1	bath-2	bath-3
$\epsilon_1$	3.021307	-1.608611	-0.268511
$V_1$	0.701389	0.518544	-0.000135
$\epsilon_2$	2.940402	-2.100353	-1.077004
$V_2$	0.337240	0.285466	-0.001323

In the next section, a large amount of DMFT calculations are conducted to construct the whole phase diagram, presenting the effect of NNN hopping on Mott MIT in two-orbital Hubbard model.

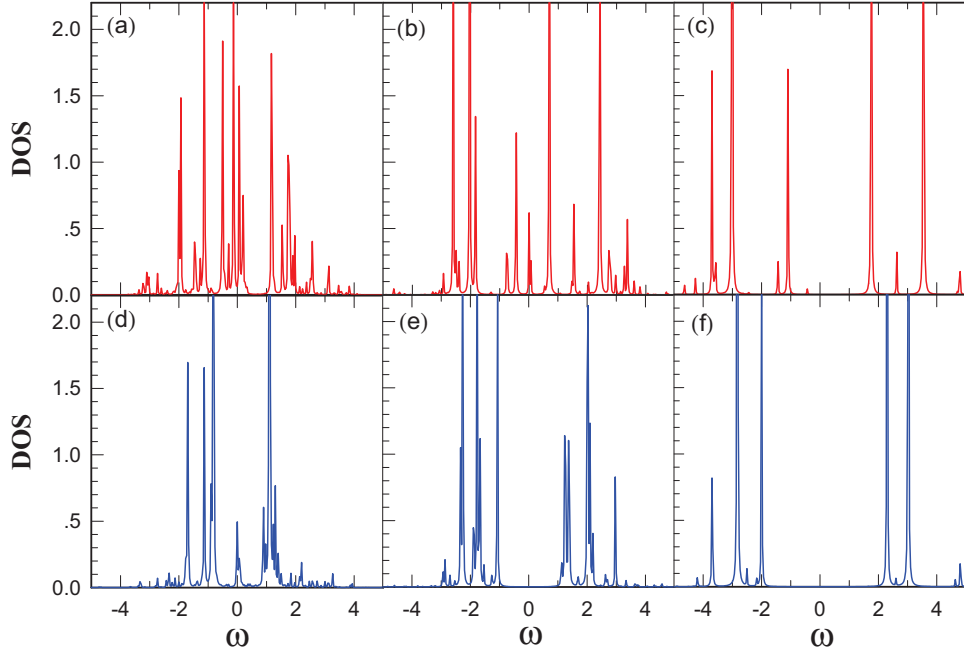


Figure 1: (Color online) Density of states of wide band (upper panel) and narrow band (lower panel) for different onsite interactions:  $U = 2.0$  ((a) and (d)),  $U = 3.0$  ((b) and (e)), and  $U = 4.5$  ((c) and (f)). The parameters of the two-orbital Hubbard model are:  $t_2/t_1 = 0.4$ ,  $K = t'_1/t_1 = t'_2/t_2 = 0.1$ ,  $J = U/4$ , and  $U' = U - 2J$ .  $t_1$  ( $t_2$ ) and  $t'_1$  ( $t'_2$ ) are nearest neighbor and next-nearest neighbor hopping integrals of the wide (narrow) band. Energies are in unit  $t_1$ , and the energy broadening factor is  $\epsilon=0.01$ .

### 3. Results

The DOS of standard Hubbard model is particle-hole symmetric at half filling. Nevertheless, in future consideration of the NNN hopping integrals, the DOS becomes asymmetric at half filling. Fig. 1 shows the DOS of the two-orbital Hubbard model with  $K = t'_1/t_1 = t'_2/t_2 = 0.1$  for different interactions  $U$ , where  $t_1$  and  $t_2$  are the NN hopping for the wide and narrow bands, and  $t'_1$  and  $t'_2$  represent the NNN hopping accordingly. The particle-hole symmetry of the DOS is broken by the NNN hopping for both the wide and narrow bands, and the asymmetry becomes more distinct in the conditions with weak interactions.

Most of the theoretical studies have paid attention to the OSMT in the systems with particle-hole symmetry at half filling [14, 15, 16, 28]. By introducing the NNN hopping, we could find out whether the OSMT exists when

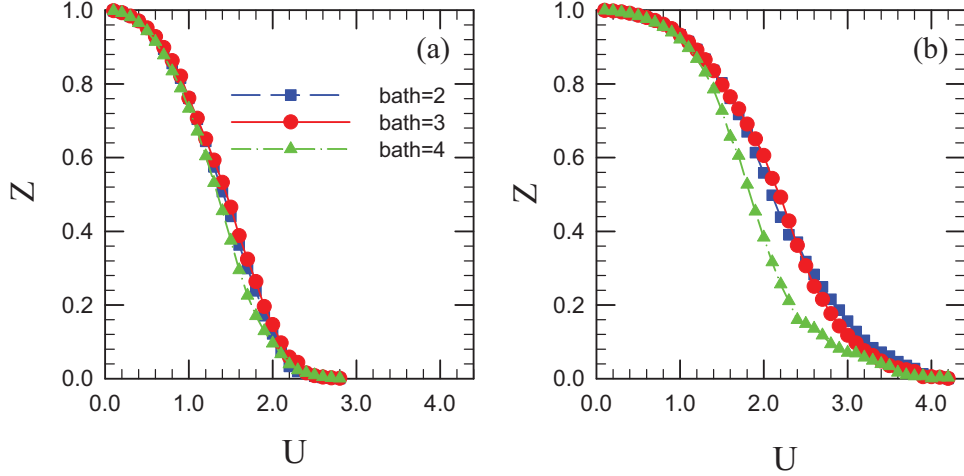


Figure 2: (Color online) Interaction dependence of the quasiparticle weight  $Z$  for the narrow band (a) and wide band (b) when  $t_2/t_1 = 0.4$ ,  $K = t'_1/t_1 = t'_2/t_2 = 0.7$ ,  $J = U/4$ , and  $U' = U - 2J$ . The results for different bath numbers  $n_b = 2, 3$  and 4 in the DMFT calculations are shown by the squares, circles and triangles, respectively. Energies are in unit  $t_1$ .

the particle-hole symmetry is broken at half filling. As shown in Fig. 1(a) and (d), resonance peaks appear at Fermi level of DOS of both the wide and narrow bands for weak interactions  $U = 2.0$ , suggesting that the two orbitals are all metallic. OSMP appears when the onsite interaction increases to  $U = 3.0$ , as shown in Fig. 1(b) and 1(e). In Fig. 1(b) the wide band is still metallic with resonance peaks at Fermi level, but a Mott gap opens around the Fermi level of the narrow band (Fig. 1(e)). Further increasing interactions to  $U = 4.5$ , both the wide and narrow bands transit to Mott insulating phase. Therefore, OSMT is still found in two-orbital Hubbard model with both NN and NNN hopping, where the DOS is asymmetric at half filling.

The critical points of OSMT could be determined precisely by studying the interaction dependence of the quasiparticle weight of each orbital ( $Z_l$ ), which is defined by

$$Z_l = \left\{ 1 - \frac{d\text{Re}\Sigma_l(\omega)}{d\omega} \Big|_{\omega=0} \right\}^{-1}, \quad (6)$$

where  $\Sigma_l(\omega)$  represents the self-energy of orbital  $l$ . Decreasing with the increasing interactions  $U$  as shown in Fig. 2, the quasiparticle weights of different orbital drops to zero successively, indicating the appearance of OSMT. When the parameters of the two-orbital Hubbard model are  $t_2/t_1 = 0.4$ ,

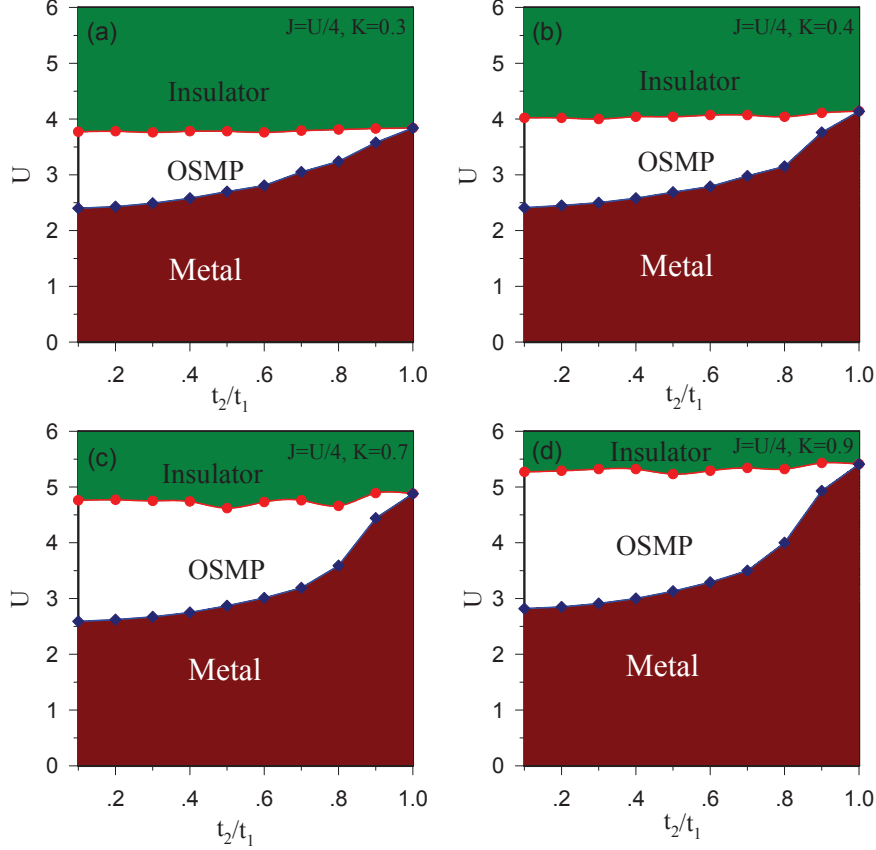


Figure 3: (Color online) Effect of the ratio between nearest neighbor hopping  $t_2/t_1$  on orbital-selective Mott transition for different next-nearest neighbor hopping ( $K = t'_1/t_1 = t'_2/t_2$ ):  $K = 0.3$  (a),  $K = 0.4$  (b),  $K = 0.7$  (c), and  $K = 0.9$  (d). The Hund's rule couplings are chosen as  $J = U/4$ , and the energies are in units of  $t_1$ .

$K = 0.7$  and  $J = U/4$ , the Mott transition happens first in the narrow band at  $U_{c2} = 2.75$ , which is much smaller than the critical value of the wide band  $U_{c1} = 4.0$ . To show the influence of the bath size on the critical points, we plot in Fig. 2 the results for different bath numbers  $n_b=2, 3$  and 4. We find that, in the two-orbital Hubbard model, the critical values of the Mott transition obtained by the cases with different bath size are very close to each other for both the narrow and wide orbitals. It is worth noting that, as  $Z_l$  drops continuously to zero, the Mott transitions are of second order for both orbitals.

In order to fully understand the effect of NNN hopping on OSMT, we



have performed a great amount calculations to obtain the phase diagrams of the two-orbital Hubbard model with different  $K$ . As mentioned above, the NNN hopping will introduce a particle-hole asymmetric DOS. We have to adjust the chemical potential to make the two orbitals are all half filled. As shown in Fig. 3, the NN hopping plays an essential rule for the appearance of OSMP, where the relationship  $t_1 \neq t_2$  should be satisfied. Because the value of the NN hopping of wide band is kept as  $t_1=1$ , the critical value  $U_{c1}$  for wide band remains unchanged in all four phase diagrams. Whereas  $U_{c2}$  for the narrow band increases continuously with the increasing  $t_2/t_1$ . Apart from the nondegeneration of the two orbitals resulted from the unequal of the NN hopping  $t_1$  and  $t_2$ , significant influence of NNN hopping on the OSMP has also been observed in Fig. 3.

On the other hand, the area of OSMP expended with the increase of  $K$ , suggesting that the NNN hopping is in favor of the OSMT. Obviously, the contribution for the extension is mainly from the elevation of the Mott transition point of the wide band  $U_{c1}$ . For example, when  $t_2/t_1 = 0.1$ ,  $U_{c1}$  increase about 45% as  $K$  increases from 0.3 to 0.9. While, the corresponding change for  $U_{c2}$  is only 12.5%. Our finding indicates that the influence of the assymmetric DOS on the OSMT is stronger in the wide band than in the narrow band. To understand this phenomena, we should consider the interplay between the multiorbital correlations and the NNN hopping rather than the effect of bandwidth ratio.

In Fig. 4, we compare the phase diagrams relied on the NNN hopping amplitude for the cases with different Hund's rule coupling ( $J$ ):  $J = U/8$ ,  $J = U/4$ , and  $J = U/2$ . As we know, Hund's coupling is responsible for strong correlations in multiorbital systems. The importance of  $J$  in promoting orbital-selective physics can be understood by recognizing that  $J$  blocks orbital fluctuations [2]. Just as expected, both  $U_{c1}$  and  $U_{c2}$  drop significantly when  $J$  increases from  $U/8$  (Fig. 4(a)) to  $J = U/2$  (Fig. 4(c)), suggesting the enhancement of the effective correlations. In order to make the computed results more clear, in Fig. 4(d) we plot the  $J/U$  dependence of  $\Delta$ , which is the difference of the critical values of the wide and narrow bands ( $\Delta = U_{c1} - U_{c2}$ ). The almost horizontal lines of  $\Delta$  indicate that the region of the OSMP is almost unchange with the increasing  $J$  in spite of the decreasing for the critical interactions for both wide and narrow band. On the other hand,  $\Delta$  for the system with NNN hopping ( $K = 1.0$ ) is near twice as large as that of the standard model with only NN hopping, suggesting that the NNN hopping has an even more obvious effect on the OSMT than the Hund's rule coupling.

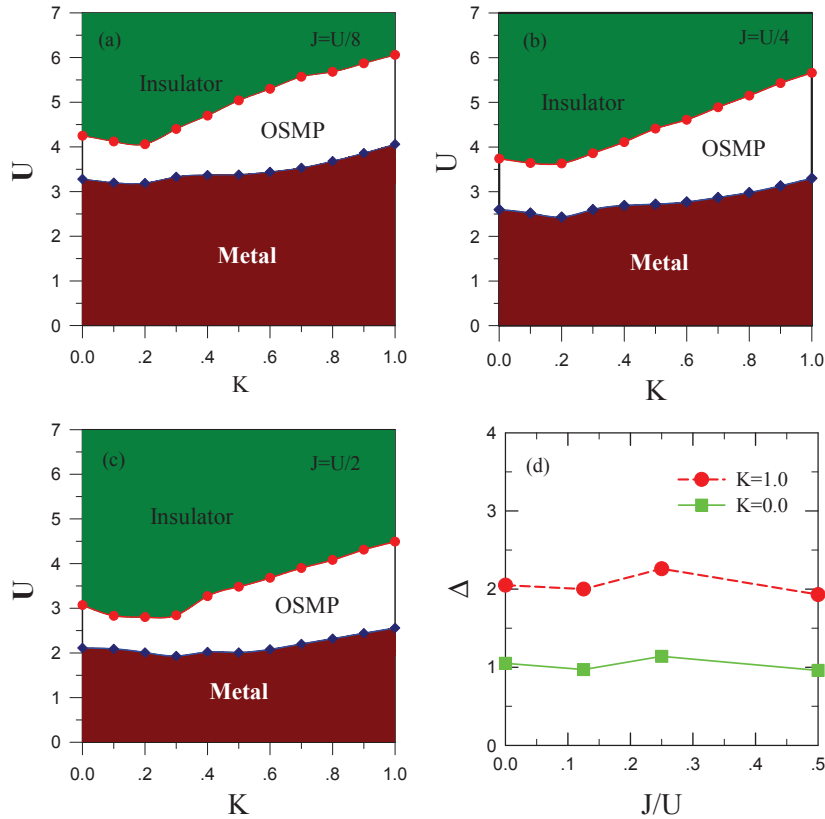


Figure 4: (Color online) Phase diagrams for the systems with different Hund's rule coupling: (a)  $J = U/8$ , (b)  $J = U/4$ , and (c)  $J = U/2$ . (d) The  $J/U$  dependence of the difference between the critical interactions of the wide and narrow band ( $\Delta = U_{c1} - U_{c2}$ ) for system with or without next-nearest neighbor hopping. The other model parameters are  $U' = U - 2J$ ,  $t_2/t_1 = 0.5$ , and the energies are in units of  $t_1$ .

#### 4. Conclusions

We emphatically study the asymmetric effect introduced by the next-nearest neighbor hopping on orbital-selective Mott transition in the two-orbital Hubbard model. We find that the asymmetric DOS introduced by the next-nearest neighbor hopping strongly influences the energetics of the Mott gap. As a result, the region of orbital-selective Mott phase increases significantly with the increasing next-nearest neighbor hopping amplitude. We also find that the orbital fluctuations are blocked with the increasing of Hund's rule coupling, leading the critical values of both narrow and wide band decrease manifestly. However, the effect of the NNN hopping on OSMT

is found to be more significant than that of the Hund's coupling.

## Acknowledgments

The computational resources utilized in this research were provided by Beijing Normal University high-performance scientific computing center. The work was supported by the NSFC of China, under Grant No. 11174036 and 11474023, the National Basic Research Program of China (Grant Nos. 2011CBA00108), and the Fundamental Research Funds for the Central Universities.

## References

- [1] G. Kotliar, S. Y. Savrasov, K. Haule, V. S. Oudovenko, O. Parcollet, and C. A. Marianetti, *Rev. Mod. Phys.* 78 (2006) 865.
- [2] A. Georges, L. de'Medici, and J. Mravlje, *Annu. Rev. Condens. Matter Phys.* 4 (2013) 137.
- [3] V. I. Anisimov, I. A. Nekrasov, D. E. Kondakov, T. M. Rice, and M. Sigrist, *Eur. Phys. J. B* 25 (2002) 191.
- [4] D. Arcon, P. Jeglic, A. Zorko, A. Potocnik, A. Y. Ganin, Y. Takabayashi, M. J. Rosseinsky, and K. Prassides, *Phys. Rev. B* 82 (2010) 140508(R).
- [5] H. Miao, Z. P. Yin, S. F. Wu, J. M. Li, J. Ma, B.-Q. Lv, X. P. Wang, T. Qian, P. Richard, L.-Y. Xing, X.-C. Wang, C. Q. Jin, K. Haule, G. Kotliar, and H. Ding, *Phys. Rev. B* 94 (2016) 201109(R).
- [6] K. Bouadim, G. G. Batrouni, and R. T. Scalettar, *Phys. Rev. Lett.* 102 (2009) 226402.
- [7] H. Lee, Y.-Z. Zhang, H. O. Jeschke, R. Valenti, and H. Monien, *Phys. Rev. Lett.* 104 (2010) 026402.
- [8] G. Kotliar, and A. E. Ruckenstein, *Phys. Rev. Lett.* 57 (1986) 1362.
- [9] E. Gull, A. J. Millis, A. I. Lichtenstein, A. N. Rubtsov, M. Troyer, and P. Werner, *Rev. Mod. Phys.* 83 (2011) 349.

- [10] A. Georges, G. Kotliar, W. Krauth, and M. J. Rozenberg, *Rev. Mod. Phys.* 68 (1996) 13.
- [11] J. Sun, Y. Liu, and Y. Song, *Acta Phys. Sin.* 64 (2015) 247101.
- [12] L. de'Medici, *Phys. Rev. B* 83 (2011) 205112.
- [13] A. Liebsch, *Phys. Rev. Lett.* 95 (2005) 116402.
- [14] A. Koga, N. Kawakami, T. M. Rice, and M. Sigrist, *Phys. Rev. Lett.* 92 (2004) 216402; A. Koga, N. Kawakami, T. M. Rice, and M. Sigrist, *Phys. Rev. B* 72 (2005) 045128.
- [15] L. de'Medici, A. Georges, and S. Biermann, *Phys. Rev. B* 72 (2005) 205124.
- [16] Y. Song and L.-J. Zou, *Phys. Rev. B* 72 (2005) 085114.
- [17] E. Jakobi, N. Blümer, and P. van Dongen, *Phys. Rev. B* 87 (2013) 205135.
- [18] Y. Song and L.-J. Zou, *Eur. Phys. J. B* 72 (2009) 59.
- [19] L. de'Medici, S. R. Hassan, M. Capone, and X. Dai, *Phys. Rev. Lett.* 102 (2009) 126401.
- [20] P. Werner, and A. J. Millis, *Phys. Rev. Lett.* 99 (2007) 126405.
- [21] M. J. Rozenberg, G. Kotliar, H. Kajueter, G. A. Thomas, D. H. Rapkine, J. M. Honig, and P. Metcalf, *Phys. Rev. Lett.* 75 (1995) 105.
- [22] R. Zitzler, N.-H. Tong, Th. Pruschke, and R. Bulla, *Phys. Rev. Lett.* 93 (2004) 016406.
- [23] M. Eckstein, M. Kollar, K. Byczuk, and D. Vollhardt, *Phys. Rev. B* 71 (2005) 235119.
- [24] R. Peters and T. Pruschke, *Phys. Rev. B* 79 (2009) 045108; R. Peters and T. Pruschke, *New J. Phys.* 11 (2009) 083022.
- [25] E. Dagotto, *Rev. Mod. Phys.* 66 (1994) 763.
- [26] M. Caffarel and W. Krauth, *Phys. Rev. Lett.* 72 (1994) 1545.

- [27] R. Chitra and G. Kotliar, Phys. Rev. Lett. 83 (1999) 2386.
- [28] L. F. Tocchio, F. Arrigoni, S. Sorella, and F. Becca, J. Phys. Condens. Matter 28 (2016) 105602 .